Spin-crossover-induced Mott transition and the other scenarios of metallization in $3d^n$ metal compounds

I. S. Lyubutin,[1] S. G. Ovchinnikov,[2] A. G. Gavriliuk,[3] and V. V. Struzhkin[4]
[1]*Institute of Crystallography, Russian Academy of Sciences, Leninsky Pr. 59, Moscow 119333, Russia*
[2]*Institute of Physics, Siberian Division, Russian Academy of Sciences, Krasnoyarsk 660036, Russia*
[3]*Institute for High Pressure Physics, RAS, 142190, Troitsk, Moscow Region, Russia*
[4]*Geophysical Laboratory, Carnegie Institution of Washington, Washington, DC 20015, USA*
(Received 3 December 2008; published 26 February 2009)

A different "Hubbard energy control" mechanism of the insulator-metal transition (IMT) in Mott-Hubbard insulators is discussed. This mechanism can be initiated by the lattice compression and it is driven by a spin crossover of $3d^5$ ions from the high-spin state to the low-spin state. The spin crossover suppresses the effective Hubbard parameter U_{eff} down to the value enabling the insulator-metal transition according to the Mott mechanism $U_{\mathrm{eff}}/W \approx 1$. The classification of possible scenarios of metallization in the other $3d^n$ metal compounds is also performed.

DOI: 10.1103/PhysRevB.79.085125 PACS number(s): 71.30.+h, 75.30.Wx, 71.27.+a, 61.50.Ks

Recently, we have reported a spin crossover of Fe^{3+} ions with simultaneous insulator-metal transition (IMT) in $BiFeO_3$ under compression.[1] Inspired by this finding, we have analyzed the pressure-induced Mott-Hubbard transition in multiorbital d^n Mott-Hubbard insulators (MHI) and found a different scenario of Mott-Hubbard IM transition which we designate as the "Hubbard energy control" mechanism in contrast to the known "bandwidth control" or "band-filling" control mechanisms.[2] This mechanism comes into effect in MHI due to the high-spin to low-spin (HS-LS) crossover in transition metal ions with d^5 configuration. Recently very similar explanation of the IMT in MnO which is another example of the d^5 system has been discussed.[3] Our further analysis indicates that this mechanism is unique for d^5 configuration and should not be effective in d^1, d^2, d^3, d^4, d^6, d^7, d^8 or d^9 configurations.

It is well known that the HS-LS spin crossover appears due to the competition between the crystal-field parameter $\Delta = 10Dq$ and the Hund's intra-atomic exchange energy J (Ref. 4). As a rule, the application of pressure increases the Δ value but does not change the parameter J. However, here we report that this competition may result in a decrease in the effective Hubbard parameter U_{eff} in compressed material due to the HS-LS spin crossover. As a result, the criterion of the IMT $U_{\mathrm{eff}}(P) = W(P)$ (W is a half of the bandwidth) comes into effect due to suppression of the U_{eff} in the low-spin state, and is much less affected by the pressure-induced changes in the bandwidth ("bandwidth control" mechanism with pressure-independent constant value of U).

We have documented the HS-LS crossover in a set of $3d^5$ systems, including $FeBO_3$,[5–7] $GdFe_3(BO_3)_4$,[8,9] $RFeO_3$ (R =La, Nd, Pr, Lu),[10–14] $Y_3Fe_5O_{12}$,[15–17] $BiFeO_3$,[1,18] and α-Fe_2O_3. All these systems show a significant decrease in the optical gap at the spin-crossover transition from nearly 3 eV, typical for insulators, to below 1 eV range, typical for semiconductors [Figs. 1(a) and 1(b)], or even to zero [Fig. 1(c)]. In the case of $Y_3Fe_5O_{12}$ and $BiFeO_3$, the optical gap drops to zero value at the spin-crossover transition, indicating possible metallization (see also Fig. 2 for $BiFeO_3$). The evidence of the spin-crossover transition in all these systems follows from the Mössbauer and nuclear forward scattering (NFS) measurements and is supported by x-ray emission spectroscopy (XES) experiments (Fig. 3). The collapse of the magnetic moment and radical drop of the local spin of $3d^5$ ions (Fig. 3) are substantial evidences for the spin-crossover transition in these systems.[6,8,10,13,16,18] The gradual tendency to metallization with pressure in all these systems finally leads to metallic state, but the scenarios are quite different. In some cases insulator-semiconductor transition is initiated by the spin crossover. The metallization in such cases occurs after further pressure increase. Such scenario is observed, for example, in $FeBO_3$ and $LaFeO_3$ [Figs. 2(a) and 2(b)].[13,19] In other cases metallization occurs directly at the spin-crossover transition in $3d^5$ system [for example, in $BiFeO_3$ and $Y_3Fe_5O_{12}$ (Refs. 1 and 15)]. The main purpose of this communication is to explain the role of the spin crossover in the Mott-type IMT, which is observed experimentally in many d^5 systems.

A good example of spin-crossover-induced Mott transition is recently observed pressure-induced metallization in $BiFeO_3$. We have found and investigated in detail the pressure-induced IMT in $BiFeO_3$ from the optical absorption spectroscopy[1] [Fig. 1(c)] and from the resistance measurements [Fig. 2(c)] both at room and low temperatures. At pressures between 45 and 55 GPa, the optical gap is decreasing to zero value, which implies an insulator-metal transition in $BiFeO_3$. The observed IMT was supported by the direct measurements of resistance R at high pressures, as it is shown in Fig. 2(c). In the range from 40 to 55 GPa we observed a drop in resistance by nearly 7 orders of magnitude. At the onset of IMT the temperature dependence of R can be fitted to the Mott formula $R = R_0 \exp(T_m/T)^{1/4}$ (Ref. 1), which is valid for the variable-range hopping.[20]

We have used several high-pressure techniques to investigate the electronic, magnetic, and structural properties of $BiFeO_3$ at high pressures in diamond anvil cells. Magnetic properties and spin states of Fe^{3+} ions were studied by the synchrotron NFS and by Fe-K_β XES. The NFS measurements at ^{57}Fe [Fig. 3(c)] clearly show a collapse of iron magnetic moments at pressures near 50 GPa.[18] The high-

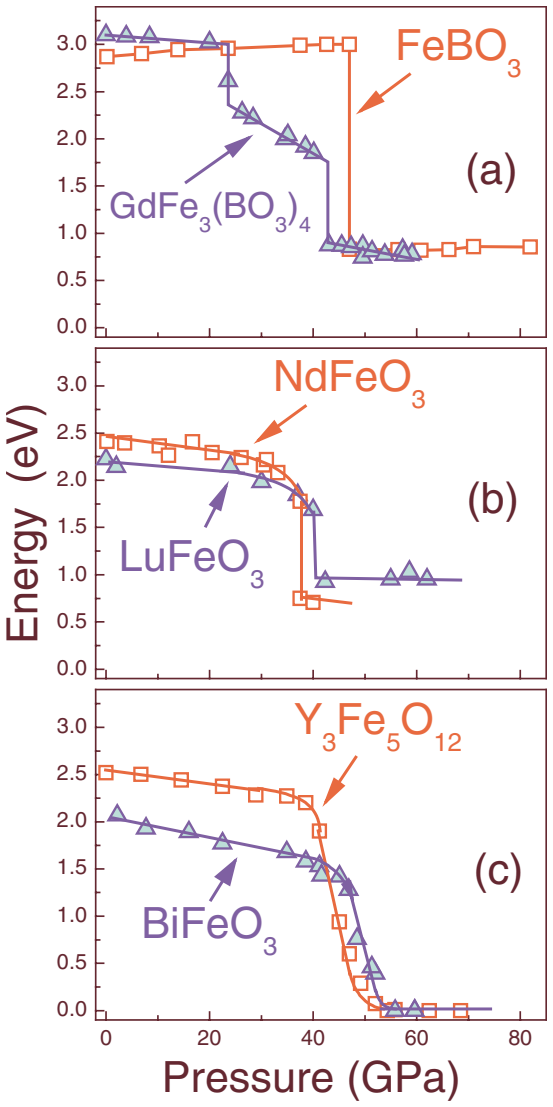

FIG. 1. (Color online) The pressure dependences of the optical gap in selected $3d^5$ systems. At the HS-LS spin transitions of Fe^{3+} ions around 50 GPa, the optical gap in $FeBO_3$, $GdFe_3(BO_3)_4$, $LuFeO_3$, and $NdFeO_3$ decreases dramatically to below 1 eV range, typical of semiconductors. In the same pressure range, the optical gaps in $BiFeO_3$ and $Y_3Fe_5O_{12}$ reveal a drop to nearly zero value indicating possible metallization.

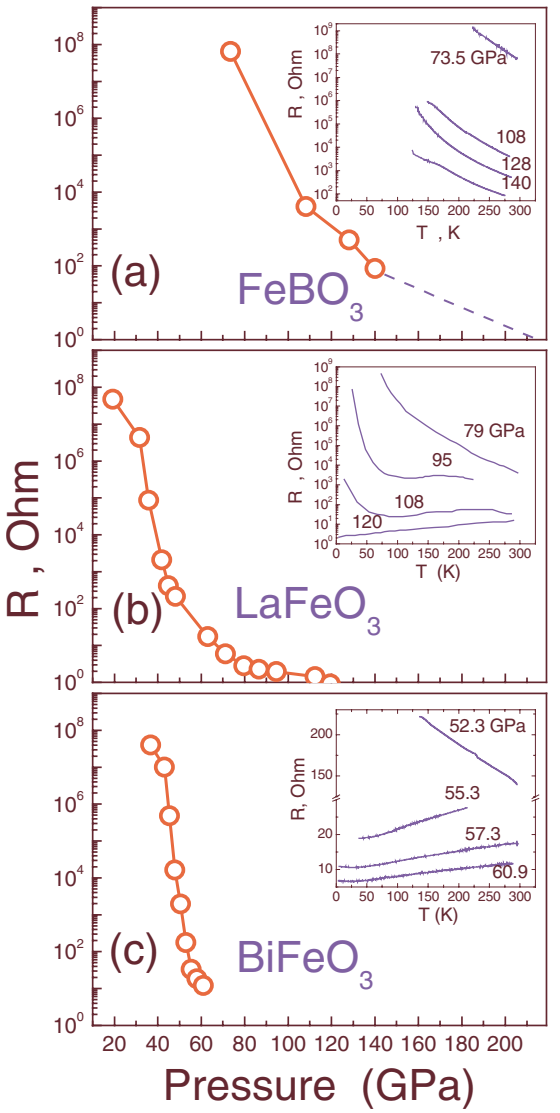

FIG. 2. (Color online) The pressure effect on resistance is shown in (a) $FeBO_3$ (Ref. 19), (b) $LaFeO_3$ (Ref. 13), and (c) $BiFeO_3$ (Ref. 1) near the HS-LS spin-crossover transitions in Fe^{3+} ions. The insets show the temperature dependence of resistance at several pressures. At the spin transition, $FeBO_3$ and $LaFeO_3$ reveal dramatic drop of resistance and transform to a semiconducting state, while in $BiFeO_3$ the insulator-metal transition is observed.

pressure XES measurements have discovered dramatic changes in the spin states of iron ion Fe^{3+} in the range from 40 to 55 GPa [inset in Fig. 3(c)].[1] These observations indicate unambiguously a spin crossover in Fe^{3+} ions from the high-spin state ($S=5/2$) to the low-spin state ($S=1/2$). Our theoretical estimates for $BiFeO_3$ show that IMT would appear at a pressure of ~370 GPa due to the band-broadening effects, while the actual critical pressure is only ~50 GPa due to the "Hubbard energy control" mechanism, as follows from our experimental data.[1] Thus, we have accumulated compelling evidence that the insulator-metal transition in $BiFeO_3$ is accompanied by the spin crossover of iron ions from the HS state to the LS state. The relation of the IMT to the spin crossover is considered below.

Mott[20] proposed the insulator model for transition metal oxides with partially filled d band. Combined with Hubbard theory,[21] this model predicts that the conductivity is suppressed by strong Coulomb interaction. For $3d^5$ configuration the effective Hubbard parameter U_{eff} of such electron repulsion is determined by the multielectron energy of d^4, d^5, and d^6 configurations,[22]

$$U_{\text{eff}}(d^5) = E_0(d^6) + E_0(d^4) - 2E_0(d^5), \tag{1}$$

where $E_0(d^n)$ are the energies of ground terms of the d^n configuration at ambient pressure. The parameter U_{eff} represents a gap between the upper Hubbard band with energy $\Omega_c = E_0(d^{n+1}) - E_0(d^n)$ and the lower Hubbard band $\Omega_v = E_0(d^n) - E_0(d^{n-1})$.[23]

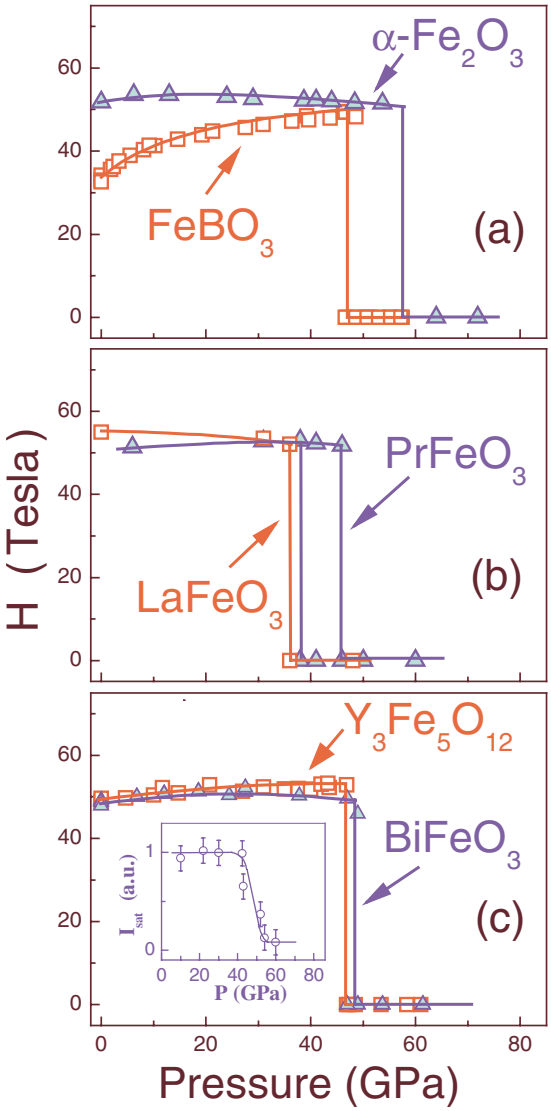

FIG. 3. (Color online) The spin-crossover transition in Fe^{3+} ions is evidenced by the pressure behavior of magnetic hyperfine fields at ^{57}Fe nuclei obtained from conventional and synchrotron Mössbauer technique in several materials: (a) $FeBO_3$ (Ref. 6), α-Fe_2O_3, (b) $LaFeO_3$ (Ref. 10), $PrFeO_3$ (Ref. 13), (c) $Y_3Fe_5O_{12}$ (Ref. 16), $BiFeO_3$ (Refs. 1 and 18). The inset in (c) shows the HS-LS spin crossover probed by x-ray Fe-K_β emission spectroscopy in $BiFeO_3$ (Ref. 1).

Here we use a single band effective Hubbard model without distinguishing between the Hubbard energy U and the charge-transfer energy E_{ct} (Ref. 24). In the case of the charge-transfer insulator, the low energy effective model is the effective Hubbard model with the energy E_{ct} instead of U. The calculation of E_{ct} is provided by the expression similar to Eq. (1) with substitution $E_0(d^{n-1})$ by $E_0(d^n\underline{L})$, where $\underline{L}$ denotes a ligand hole. We should mention that in order to construct a microscopic theory of IMT in a given crystal one has to discuss orbital degeneracy of $3d$ electrons, its splitting in the crystal field of the proper symmetry (usually distorted from the cubic one), and details of the band structure.[25–27] Here we restrict consideration to a semiquantitative approach in the framework of the effective Hubbard model to elucidate the "Hubbard energy control" mechanism in the simplest way. We have a good experience constructing the effective Hubbard model for the low energy physics from our calculations the electronic structure of copper oxides.[28] The kinetic energy of electrons is determined by the width of the d band $2W$. In this case the fundamental gap of the insulator is equal to $(U_{\text{eff}}-W)$, and the criterion of the transition from the insulating to the metallic state is $W\sim U_{\text{eff}}$ (Ref. 20).

As it follows from the Tanabe-Sugano calculations,[4] at high pressures the d^4, d^5, and d^6 configurations reveal spin crossovers at the increase in the crystal-field parameter Δ. Below we will show that for d^5 ions the effective Hubbard parameter U_{eff} is decreased with increasing pressure.

Our calculations (see the details in the Appendix) reveal that there are three regions of the pressure-induced changes in the parameter Δ/J which correspond to different ground states of d^n terms:

(i) At $\Delta/J<2$ all d^4, d^5, and d^6 configurations are in HS state.

(ii) At $2\leq\Delta/J\leq 3$ the d^4 and d^5 terms are in HS state and the d^6 term is in LS state.

(iii) And finally, at $\Delta/J>3$ the d^4 term is in intermediate spin (IS) state; the d^5 and d^6 terms are in LS state. In these regions, the different behavior of the parameter U_{eff} is given by

$$U_{\text{eff}}(d^5)=\begin{cases}U(d^5)+4J-\Delta & \text{at } \Delta/J<2\\ U(d^5)+8J-3\Delta & \text{at } 2\leq\Delta/J\leq 3\\ U(d^5)-J & \text{at } \Delta/J>3.\end{cases} \quad (2)$$

Here $U(d^5)=E_C(d^6)+E_C(d^4)-2E_C(d^5)$, where $E_C(d^n)$ is the part of the Coulomb energy for d^n configuration independent of the total spin. It is determined by a distribution of n electrons over five d orbitals for a given configuration and includes different intraorbital and interorbital Coulomb matrix elements.

Both the crystal-field parameter Δ and the bandwidth W grow with pressure, and we assume that this change is linear in a limited pressure range: $W(P)=W_0+\alpha_W P$, $\Delta(P)=\Delta_0+\alpha_\Delta P$. Thus we can estimate pressure dependencies of U_{eff} and W as it is shown in Fig. 4. The sharp bends of the U_{eff} line at the points P_1^{cross} and P_2^{cross} in Fig. 4 correspond to the spin crossover for d^6, d^4, and d^5 configurations, respectively, while the crossover points of the U_{eff} and W lines at P_1, P_2, P_3, and P_4 correspond to IMT. It is obvious that in the pressure range $P_1^{\text{cross}}\leq P\leq P_2^{\text{cross}}$ the linear slopes of Δ and W should be renormalized to larger values because in this region there is anomaly in volume decrease of d^n ion due to spin crossover. This renormalization could be taken into account as $\alpha_W\rightarrow y\alpha_W$, $\alpha_\Delta\rightarrow y\alpha_\Delta$ where parameter $y>1$ (the detailed discussion may be found in the Appendix).

Depending on the W_0 and α_W values, there are three possible scenarios of the IMT (Fig. 4):

(1) Both W_0 and α_W are large (line 1 in Fig. 4). In this case IMT occurs in the HS states of d^4, d^5, and d^6 configurations. The "Hubbard energy control" mechanism does not change substantially the critical pressure as determined by the "bandwidth control" mechanism (e.g., point P_1 in Fig. 4).

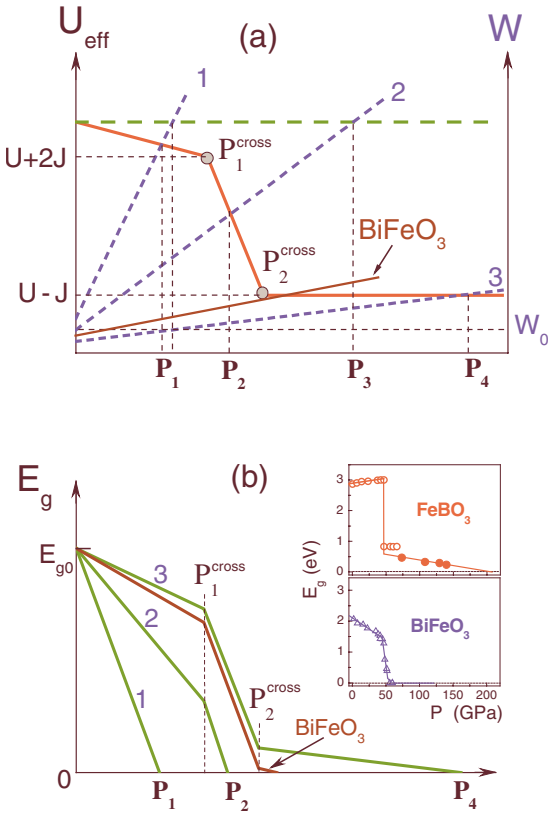

FIG. 4. (Color online) (a) A diagram elucidating the Hubbard–energy control mechanism of the Mott-Hubbard transition. The dependencies of U_{eff} (solid red lines) and W (dashed blue lines labeled 1, 2, and 3) on pressure are drawn for the d^5 configuration taking into account the spin crossover effects. Dashed green horizontal line corresponds to the constant level U_0 when U_{eff} is independent of P. On the $U_{\text{eff}}(P)$ curve, the points P_1^{cross} and P_2^{cross} correspond to the spin crossover for d^6 and for d^4, d^5 configurations, respectively, while the crosses of the $U_{\text{eff}}(P)$ and $W(P)$ lines at the P_1, P_2, and P_4 points correspond to IMT. Three different $W(P)$ lines 1, 2, and 3 correspond to different dependence of W on pressure ($\alpha_{W1} > \alpha_{W2} > \alpha_{W3}$). Points P_1, P_2, and P_4 are the pressures of the insulator-metal Mott-Hubbard transitions in the Hubbard–energy control mechanism. (b) The types of pressure dependencies of the band gap E_g as a result of different scenarios from the theoretical model in part (a). The case of $BiFeO_3$ is indicated by an arrow. The inset shows the experimental examples of pressure dependence of the gap for $BiFeO_3$ and $FeBO_3$ [filled points correspond to the thermo-activating gap from resistivity measurements (Ref. 19); open symbols correspond to the optical gap from optical absorption]. The case of $FeBO_3$ is a good example of scenario 3 from part (a).

In this case the "bandwidth control" is the governing mechanism consistent with previous consideration.[29]

The semiquantitative IMT criterion is $U=xW$, and the numerical parameter x depends on the crystal lattice, details of the band structure, and the single particle density of states, and approximations. In the initial Hubbard III solution $x=1.74$ (Ref. 30), while $x=3$ in the dynamical mean-field theory (DMFT) (Ref. 31) and $x=2.3$ in the cluster DMFT calculations.[32] In all calculations $x \sim 1$ that is most important in our approach. Below we will use the $x=2.3$ value in numerical estimations.

(2) Both W_0 and α_W are small (line 3 in Fig. 4). At these W_0 and α_W values, IMT may occur when both d^5 and d^6 configurations are in the LS states while d^4 is in the IS state (see point P_4 in Fig. 4). In this situation, U_{eff} is less than $U_0=U_{\text{eff}}(P=0)$ by the factor of $(5J-\Delta)$. For Fe^{3+} ion, the typical value of J is 0.8 eV, and Δ is about 1.0–1.5 eV.[23] Therefore, before IMT, the decrease in U_{eff} is about 2.5–3 eV. In this case the spin crossover in d^5 configuration (point P_2^{cross} in Fig. 4) will result in an insulator-semiconductor transition. The semiconducting state persists up to the point $xW(P)=U_{\text{eff}}$ where IMT takes place (at P_4 in Fig. 4). At pressures above this point a metallic state occurs. We have observed this scenario experimentally in $FeBO_3$ [Refs. 5 and 6 and inset in Fig. 4(b)], $GdFe_3(BO_3)_4$ (Refs. 8 and 9) and $RFeO_3$ (R=Lu,Nd) (Ref. 14). Our theoretical estimates for the pressure behavior and for the critical pressure of metallization are in good agreement with the experimental data obtained for $FeBO_3$ (Ref. 19) [see also Fig. 2(a), inset in Fig. 4(b), and the Appendix].

(3) The line 2 in Fig. 4 corresponds to intermediate values of W_0 and α_W. In this case the IMT occurs at HS states of the d^4 and d^5 terms and LS state of the d^6 term (point P_3 in Fig. 4). The crossing of $W(P)$ line 2 with the constant level U_0 (when U_{eff} is independent of P) at the point P_3 indicates a possible IMT due to the "bandwidth control" mechanism. However the actual IMT occurs at lower pressure due to the "Hubbard energy control" at the P_2 value, which is much lower than P_3. The estimates of the IMT pressure for $BiFeO_3$ are in an excellent agreement with experimental data.[1] The estimates for the "bandwidth control" scenario give the IMT pressure about 370 GPa, while due to the spin-crossover effects (the "Hubbard energy control" mechanism) it occurs at 55 GPa [see Fig. 2(c), inset in Fig. 4(b), and Appendix].

The insulator-metal transition of Mott type was observed in $BiFeO_3$ at high pressures above 55 GPa, concomitant with the HS-LS crossover of Fe^{3+} ions. The analysis of the data elucidates a different mechanism of IMT in Mott-Hubbard insulators. This mechanism can be brought into effect by high pressure and it is driven by the spin crossover of d^5 ions from the high-spin state to the low-spin state. We have shown that the spin crossover suppresses the effective Hubbard parameter U_{eff} below the IMT threshold $U_{\text{eff}}/W \approx 1$. We dubbed the IMT mechanism as the "Hubbard energy control" mechanism in addition to the known "bandwidth control" and "doping-control" mechanisms.

We believe that this mechanism is also relevant for other $3d^5$ transition-metal compounds such as $FeBO_3$,[5–7] $GdFe_3(BO_3)_4$,[8,9] $RFeO_3$ (R=La,Nd,Pr,Lu),[10–14] $Y_3Fe_5O_{12}$,[15–17] α-Fe_2O_3,[33,34] Fe_3O_4,[35] MnO (Refs. 36 and 37) where the spin crossover was found along with insulator-metal or insulator-semiconductor transitions (see also Refs. 11 and 34). Of course, in a given oxide all mechanisms work together, and our consideration of different scenarios in Fig. 4 is revealing the different possibilities. The IMT may occur simultaneously with the spin crossover, as it occurs in our case (3) (line 2 in Fig. 4) and was pointed out in Ref. 3 for a MnO, or it may follow after the spin crossover due to decrease in the effective Hubbard parameter U_{eff} as we have shown here for $BiFeO_3$. According to Ref. 38, the similar decrease in the single particle gap and the forthcoming spin crossover take place in α-Fe_2O_3.

TABLE I. Behavior of U_{eff} for different d^n ions at increase in crystal-field parameter Δ.

Type of d^n ion	U_{eff} for different values of crystal-field parameter Δ		
	$\Delta/J<2$	$2\leq\Delta/J\leq 3$	$3\leq\Delta/J$
U_{eff} (d^5)	$U(d^5)+4J-\Delta$	$U(d^5)+8J-3\Delta$	$U(d^5)-J$
U_{eff} (d^6)	$U(d^6)-J$	$U(d^6)-7J+3\Delta$	$U(d^6)-J+\Delta$
	$\Delta/J<3$		$3<\Delta/J$
U_{eff} (d^3)	$U(d^3)-J+\Delta$		$U(d^3)+2J$
	$\Delta/J<2$		$2<\Delta/J$
U_{eff} (d^8)	$U(d^8)-J+\Delta$		$U(d^8)+J$
U_{eff} (d^1,d^9)	$U(d^1,d^9)-J$ (no spin crossovers, U_{eff} is independent of Δ)		
U_{eff} (d^2,d^4,d^7)	$U(d^2,d^4,d^7)-J$ (U_{eff} is constant at all values of Δ)		

It is significant that from the thermodynamic point of view, the spin crossover is not a phase transition because there is no thermodynamic order parameter that differentiates the HS and LS states. The value of magnetization changes at the spin crossover but this is a quantitative change, not qualitative. However at $T=0$ K the spin crossover is a quantum critical point according to the general theory.[39] For example, there should be a jump of spin entropy S at very low temperatures near the critical pressure, because for the HS state $\Delta S\sim\ln 6$ while for the LS state $\Delta S\sim\ln 2$. Other examples of quantum critical points induced by pressure in heavy-fermion compounds such as $CeIn_3$ and UGe_2 are given in Ref. 40.

In a recent theoretical study[41] it was found that in d^4, d^6, d^7, and d^8 systems spin-crossover effects do not have such dramatic effect on the effective Hubbard parameter U_{eff}. We summarized theoretical considerations in Table I. The details of the calculations could be found in Ref. 41 and in the Appendix.

In summary, our findings of "Hubbard-energy controlled" IMT in d^5 systems present a unique situation of the interplay between local parameters in the multiorbital Hubbard model and the collective behavior of the charge carriers in the system at the onset of the insulator-metal transition, which has no analogs in other d^n configurations.

The use of the Advanced Photon Source is supported by the U.S. Department of Energy, Basic Energy Sciences, Office of Science, under Contract No. W-31-109-EN. This work was supported by the DOE Grant No. DE-FG02-02ER45955, by the Russian Foundation for Basic Research Grants No. 08-02-00897a, No. 07-02-00226, and No. 07-02-00490-a, and by the Russian Academy of Sciences Projects "Strongly correlated electronic systems" and "Nanotechnology and Nanomaterials" (Grant No. 27-4.1.10).

APPENDIX

1. Details of theoretical estimations of U_{eff} for different d^n cases

In Tanabe-Sugano calculations, all intra-atomic Coulomb matrix elements have been considered and all multiplets for a given d^n configuration have been obtained. We will simplify these calculations assuming that for all states of d^n configuration spin-independent Coulomb matrix elements are the same and the difference in the energy for different spin states stems from two factors: (i) each pair of parallel spins gains the Hund exchange energy J compared to the antiparallel spin pair; (ii) cubic crystal field $\Delta=10Dq$ splits the atomic single electron d level into the t_{2g} and e_g levels with the energies $-4Dq$ and $+6Dq$, respectively. Within this very simple approach we can write down analytically the energy of different spin states and obtain the criteria for spin crossovers in agreement with the Tanabe-Sugano calculations.[35] In this approximation we cannot obtain a full set of terms with given spin, so it cannot be used for spectroscopy. Nevertheless this approach appears to be very useful to study spin crossovers and their effect on the electronic structure. Thus for d^5 configuration we can write down the HS and LS terms energy as the following:

$$E_{\text{HS}}(d^5)=E_C(d^5)-10J,$$

$$E_{\text{LS}}(d^5)=E_C(d^5)-20Dq-4J, \tag{A1}$$

where $E_C(d^5)$ is the spin-independent part of the Coulomb energy for d^5 configuration. To calculate the effective U we also need the energies for d^4 and d^6 configurations that can be written as

$$E_{\text{HS}}(d^4)=E_C(d^4)-6Dq-6J,$$

$$E_{\text{IS}}(d^4)=E_C(d^4)-16Dq-3J, \tag{A2}$$

$$E_{\text{HS}}(d^6)=E_C(d^6)-4Dq-10J,$$

$$E_{\text{LS}}(d^6)=E_C(d^6)-24Dq-6J. \tag{A3}$$

With these energies it is straightforward to get the U_{eff} as it is given for d^5 configuration in Eq. (2).

For d^2, d^4, and d^7 configurations the U_{eff} does not depend on pressure:

$$U_{\text{eff}}(d^2,d^4,d^7) = U(d^2,d^4,d^7) - J. \tag{A4}$$

For d^6 configuration the U_{eff} may grow with pressure:

$$U_{\text{eff}}(d^6) = \begin{cases} U(d^6) - J & \text{at } \Delta/J < 2 \\ U(d^6) - 7J + 3\Delta & \text{at } 2 \le \Delta/J \le 3 \\ U(d^6) - J + \Delta & \text{at } \Delta/J > 3. \end{cases} \tag{A5}$$

For d^8 configuration the U_{eff} first grows with pressure and then it goes to saturation:

$$U_{\text{eff}}(d^8) = \begin{cases} U(d^8) - J + \Delta & \text{at } \Delta/J < 2 \\ U(d^8) + J & \text{at } \Delta/J < 2. \end{cases} \tag{A6}$$

For d^1 and d^9 configurations spin crossovers do not appear and U_{eff} is independent of pressure.

2. Corrections to d^5 case

Between P_1^{cross} and P_2^{cross} the experimental data show a strong increase in the lattice compressibility, and to take this fact into account we renormalize the pressure derivatives of the bandwidth and crystal field in this region of pressure as $\alpha_W \to y\alpha_W$, $\alpha_\Delta \to y\alpha_\Delta$ with parameter $y > 1$.

At relatively small pressures, the insulator gap $E_g = U - W$ is far from zero, but near the IMT it is $E_g = U - U_c$, where $U_c = xW$. The pressure dependence of the gap is given by

$$E_g = \begin{cases} E_{g0} - k_1 P & \text{at } P < P_1^{\text{cross}} \\ E_g(P_1^{\text{cross}}) - k_2(P - P_1^{\text{cross}}) & \text{at } P_1^{\text{cross}} < P < P_2^{\text{cross}} \\ E_g(P_2^{\text{cross}}) - k_3(P - P_2^{\text{cross}}) & \text{at } P > P_2^{\text{cross}}. \end{cases} \tag{A7}$$

Here E_{g0} is the gap value at $P=0$, $k_1 = \alpha_W + \alpha_\Delta$ and $k_2 = y(x\alpha_W + 3\alpha_\Delta)$, $k_3 = x\alpha_W$.

3. Applicability of the linear approximation for pressure dependencies of W and Δ

Linear changes in the bandwidth and crystal field changes at small pressure result from small changes in the lattice parameters (at least up to 50 GPa). At higher pressures nonlinear contribution becomes more important. In this paper we take it into account by renormalization of the baric derivatives in the crossover region 40–55 GPa; in other words we use two linear dependences with different slopes. In the crossover region structural deformations occur due to the change in the ionic radii which has nothing in common with the power dependence of the Hamiltonian parameters on interatomic distance for a fixed d^n configuration.

4. Numerical estimates for $FeBO_3$

The model parameters calculated for $FeBO_3$ are the following:[23] $U_0 = 4.2$ eV, $J = 0.8$ eV, $\Delta_0 = 1.5$ eV, and $W_0 = 0.36$ eV. It gives $\alpha_W = 0.002$ eV/GPa, and $\alpha_\Delta = 0.02$ eV/GPa. Thus the spin crossover occurs at $P = P_2^{\text{cross}} = (3J - \Delta_0)/\alpha_\Delta \approx 45$ GPa, while the IMT point at P_4 is given by $P_4 = (U_0 - 5J + \Delta_0 - xW_0)/x\alpha_W \approx 190$ GPa. These estimates of the critical pressures are in good agreement with the experimental data obtained for $FeBO_3$ (Ref. 29).

5. Numerical estimates for $BiFeO_3$

Our analysis of the experimental data (see Figs. 1–3) reveals that in $BiFeO_3$ the IMT scenario corresponds to the case (3) with the $W(P)$ line crossing the $U_{\text{eff}}(P)$ line very close to the spin crossover point P_2^{cross} (see brown line labeled $BiFeO_3$ in Fig. 4). The IMT occurs just after the spin crossover as the result of a sharp decrease in the effective Hubbard parameter U_{eff} due to the crossover.

We take the typical values of $U_0 = 3.55$ eV and $W_0 = 1$ eV. Then from four experimental parameters $k_1 = 0.0125$ eV/GPa [see Eq. (A7)], two spin crossover values $P_1^{\text{cross}} = 40$ GPa, $P_2^{\text{cross}} = 48$ GPa, and the IMT point $P_{\text{IMT}} = 55$ GPa we have found four unknown parameters y, Δ_0, α_W, and α_Δ. These parameters are $\Delta_0 = 1.16$ eV, $\alpha_W = 0.0015$ eV/GPa, $\alpha_\Delta = 0.011$ eV/GPa, and $y = 2.35$. We have calculated the $k_2 = y(x\alpha_W + 3\alpha_\Delta)$ value and we have obtained $k_2 = 0.086$ eV/GPa in agreement with the experimental value 0.10 eV/GPa, which serves as an independent confirmation of the consistency of our parameters.

Thus in $BiFeO_3$, the IMT induced by the Hubbard energy control mechanism occurs at

$$P_{\text{IMT}} = (U - J - xW_0)/yx\alpha_W \approx 55 \text{ GPa}, \tag{A8}$$

while the bandwidth control mechanism results in the IMT at

$$P_{\text{IMT}} = (U - xW_0)/x\alpha_W \approx 370 \text{ GPa}. \tag{A9}$$

[1] A. G. Gavriliuk, V. V. Struzhkin, I. S. Lyubutin, S. G. Ovchinnikov, M. Y. Hu, and P. Chow, Phys. Rev. B **77**, 155112 (2008).
[2] M. Imada, A. Fujimori, and Y. Tokura, Rev. Mod. Phys. **70**, 1039 (1998).
[3] J. Kuneš, A. V. Lukoyanov, V. I. Anisimov, R. T. Scalettar, and W. E. Pickett, Nature Mater. **7**, 198 (2008).
[4] Y. Tanabe and S. Sugano, J. Phys. Soc. Jpn. **9**, 753 (1954).
[5] A. G. Gavriliuk, I. A. Trojan, S. G. Ovchinnikov, I. S. Lyubutin, and V. A. Sarkisyan, JETP **99**, 566 (2004).
[6] A. G. Gavriliuk, I. A. Trojan, I. S. Lyubutin, S. G. Ovchinnikov, and V. A. Sarkissian, JETP **100**, 688 (2005).
[7] A. G. Gavriliuk, I. A. Trojan, R. Boehler, M. Eremets, A. Zerr, I. S. Lyubutin, and V. A. Sarkissyan, JETP Lett. **75**, 23 (2002).
[8] A. G. Gavriliuk, S. A. Kharlamova, I. S. Lyubutin, I. A. Troyan, S. G. Ovchinnikov, A. M. Potseluiko, M. I. Eremets, and R. Boehler, JETP Lett. **80**, 426 (2004).
[9] I. S. Lyubutin, A. G. Gavriliuk, V. V. Struzhkin, S. G. Ovchinnikov, S. A. Kharlamova, L. N. Bezmaternykh, M. Hu, and P. Chow, JETP Lett. **84**, 518 (2007).
[10] G. R. Hearne, M. P. Pasternak, R. D. Taylor, and P. Lacorre, Phys. Rev. B **51**, 11495 (1995).
[11] A. G. Gavriliuk, G. N. Stepanov, I. S. Lyubutin, A. S. Stepin, I. A. Ttojan, and V. A. Sidorov, Hyperfine Interact. **126**, 305 (2000).

[12] A. G. Gavrilyuk, G. N. Stepanov, I. S. Lyubutin, A. S. Stepin, I. A. Troyan, V. A. Sidorov, B. Palosz, S. Stel'makh, and M. Winzenick, JETP **90**, 330 (2000).
[13] W. M. Xu, O. Naaman, G. K. Rozenberg, M. P. Pasternak, and R. D. Taylor, Phys. Rev. B **64**, 094411 (2001).
[14] A. G. Gavriliuk, I. A. Trojan, R. Boehler, M. I. Eremets, I. S. Lyubutin, and N. R. Serebryanaya, JETP Lett. **77**, 619 (2003).
[15] A. G. Gavriliuk, V. V. Struzhkin, I. S. Lyubutin, and I. A. Trojan, JETP Lett. **82**, 603 (2005).
[16] I. S. Lyubutin, A. G. Gavriliuk, I. A. Trojan, and R. A. Sadykov, JETP Lett. **82**, 702 (2005).
[17] A. G. Gavriliuk, V. V. Struzhkin, I. S. Lyubutin, M. I. Eremets, I. A. Trojan, and V. V. Artemov, JETP Lett. **83**, 37 (2006).
[18] A. G. Gavriliuk, V. V. Struzhkin, I. S. Lyubutin, M. Y. Hu, and H. K. Mao, JETP Lett. **82**, 224 (2005).
[19] I. A. Troyan, M. I. Eremets, A. G. Gavrilyuk, I. S. Lyubutin, and V. A. Sarkisyan, JETP Lett. **78**, 13 (2003).
[20] N. F. Mott, *Metal-insulator Transitions* (Taylor and Francis, London, 1990).
[21] J. C. Hubbard, Proc. R. Soc. London, Ser. A **276**, 238 (1963).
[22] J. Zaanen and G. A. Sawatzky, J. Solid State Chem. **88**, 8 (1990).
[23] S. G. Ovchinnikov, J. Magn. Magn. Mater. **300**, 243 (2006).
[24] J. Zaanen, G. A. Sawatzky, and J. W. Allen, Phys. Rev. Lett. **55**, 418 (1985).
[25] O. Gunnarsson, E. Koch, and R. M. Martin, Phys. Rev. B **54**, R11026 (1996).
[26] E. Pavarini, S. Biermann, A. Poteryaev, A. I. Lichtenstein, A. Georges, and O. K. Andersen, Phys. Rev. Lett. **92**, 176403 (2004).
[27] P. Werner and A. J. Millis, Phys. Rev. Lett. **99**, 126405 (2007).
[28] M. M. Korshunov, V. A. Gavrichkov, S. G. Ovchinnikov, I. A. Nekrasov, Z. V. Pchelkina, and V. I. Anisimov, Phys. Rev. B **72**, 165104 (2005).
[29] R. E. Cohen, I. I. Mazin, and D. G. Isaak, Science **275**, 654 (1997).
[30] J. Hubbard, Proc. R. Soc. London, Ser. A **281**, 401 (1964).
[31] A. Georges, G. Kotliar, W. Krauth, and M. Rozenberg, Rev. Mod. Phys. **68**, 13 (1996).
[32] O. Parcollet, G. Biroli, and G. Kotliar, Phys. Rev. Lett. **92**, 226402 (2004).
[33] M. P. Pasternak, G. K. Rozenberg, G. Y. Machavariani, O. Naaman, R. D. Taylor, and R. Jeanloz, Phys. Rev. Lett. **82**, 4663 (1999).
[34] I. S. Lyubutin, A. G. Gavriliuk, and V. V. Struzhkin, in *Materials Research at High Pressure*, edited by A. F. G. M. R. Manaa, R. J. Hemley, and R. Bini (Materials Research Society, Warrendale, PA, 2007), Vol. 987, p. 167.
[35] E. R. Morris and Q. Williams, J. Geophys. Res. **102**, 18139 (1997).
[36] D. Kasinathan, J. Kuneš, K. Koepernik, C. V. Diaconu, R. L. Martin, I. D. Prodan, G. E. Scuseria, N. Spaldin, L. Petit, T. C. Schulthess, and W. E. Pickett, Phys. Rev. B **74**, 195110 (2006).
[37] D. Kasinathan, K. Koepernik, and W. E. Pickett, New J. Phys. **9**, 235 (2007).
[38] J. Kunes, D. M. Korotin, M. A. Korotin, V. I. Anisimov, and P. Werner, arXiv:0810.2864 (unpublished).
[39] S. Sachdev, Nat. Phys. **4**, 173 (2008).
[40] S. S. Saxena *et al.*, Nature (London) **406**, 587 (2000).
[41] S. G. Ovchinnikov, JETP **107**(1), 140 (2008).